Improving Global Surface and Internal Tides through Two-Way Coupling with High Resolution Coastal Models

PI Maarten Buijsman
Department of Marine Science
University of Southern Mississippi
Stennis Space Center, MS 39529
Phone: (228) 688-2385; Fax: (228)-688-1121
E-mail: maarten.buijsman@usm.edu
Award Number: N00014-15-1-2288

co-PI Brian K. Arbic
Department of Earth and Environmental Sciences, University of Michigan,
Ann Arbor, MI, 48109
Phone: (734) 615-4941; Fax: (734) 763-4690
Email: arbic@umich.edu
Award Number: N00014-15-1-2288

co-PI Alan J. Wallcraft
NRL Code 7323
Stennis Space Center, MS 39529-5004
Phone: (228) 688-4813; Fax: (228) 688-4759
Email: Alan.Wallcraft@nrlssc.navy.mil
Award Number: N00014-15-WX-01744

co-PI James Richman
Center for Ocean-Atmospheric Prediction Studies, Florida State University
2000 Levy Avenue, Building A, Suite 292
Tallahassee, FL 32306-2741
Phone: (850) 644-4581; Fax: (850) 644-4841
james.richman.ctr@nrlssc.navy.mil

co-PI Jay Shriver
NRL Code 7323
Stennis Space Center, MS 39529-5004
Phone: (228) 688-4625; Fax: (228) 688-4759
Email: Alan. jay.shriver@nrlssc.navy.mil
Award Number: N00014-15-WX-01744

LONG-TERM GOALS

The Navy produces weekly global forecasts of the state of the ocean, updated daily. These forecasts are used to aid decision making and to provide boundary conditions for higher resolution regional models. Tides play an important role in the high frequency variability of the ocean, modulating acoustic propagation and loss. Tidal currents affect small boat and diver operations. At present, the barotropic tides are added to the boundary conditions to force tidal motions in the regional models. However, this approach fails to adequately forecast the internal tides. The present plans call for the Navy to transition a global 1/25° forecast system with embedded tides at the end of FY17. The current global 1/25° model has large errors for tides in the coastal ocean.

The long-term goals are to increase the accuracy of the tides in the global ocean forecast model using a two-way nesting technique. This technique has a significant advantage over the current one-way nesting approach with significantly lower cost than increasing the model resolution everywhere. Thus, the proposed research will advance the Navy forecasting capacity and improve the information provided to decision makers.

OBJECTIVES

In recent years much progress has been made with implementing, validating, and improving tides in global HYCOM. However, the root-mean square errors between predicted and observed tides in the North Atlantic remain much larger than in other ocean basins. These errors may be attributed to complex coastal shelf geometry on the Hudson and European shelves that is poorly resolved in 1/12.5º and 1/25º global HYCOM. The North Atlantic has strongly resonant tides that are very sensitive to coastal geometry. The tides near the coast are impacted by the incoming tides from the deep ocean. Additionally, the resonant tides over the shelf impact the deep ocean tides.

The objectives of this study are to improve the surface tides, and implicitly the baroclinic tides in HYCOM, through a two-way coupling of the coarse resolution parent HYCOM model with high-resolution nested coastal models. For this purpose, we will use the two-way coupling method OASIS.

APPROACH

Global HYCOM uses a tripole grid that is Mercator (square) south of 47º N. In order to accurately resolve the coastal shelf geometry and bathymetry, and hence the coupling between open-ocean and coastal tides in highly resonant regions, grid spacings smaller than 1/25º are required. To accomplish this we propose to nest coastal (HYCOM) models having a very high horizontal resolution of about 1 km inside global HYCOM. We will use OASIS, a Fortran package that facilitates two-way coupling of two concurrent running simulations. The two-way coupling is needed to allow surface and internal tides to radiate from the coastal model into the parent model, and vice versa. Since the resonance signal is large and basin-wide, we anticipate a significant difference in the two-way coupled case.

In a first step we will perform the coupling for tide-only, barotropic (one layer) HYCOM simulations. The coupling will occur between the 1/25° parent grid and the 1/75° high-resolution nest. These experiments will be compared with a global 1/75° barotropic simulation. If time permits, we will also execute the same coupling experiment, but for a 41-layer HYCOM simulation with realistic tides and atmospheric forcing.

Initially we will nest higher resolution models of the Hudson and European shelves, North Atlantic regions that are highly resonant and that contribute substantially to the large RMS elevation errors in the North Atlantic. If this is successful, the two-way coupling technique can be applied to other regions as well.

The proposed experiments are summarized below:

- Apply OASIS 1/75° nests to Hudson Strait and European shelf embedded in the 1/25°, tide-only, barotropic (one layer) HYCOM parent simulations.
  GOAL: -confirm that OASIS handles tides
  -correctly capture the resonances in the North Atlantic

- Perform global 1/75° barotropic simulations
  GOAL: compare with two-way nesting (1/75° nest in 1/25° global model)

- Apply the OASIS 1/75° nests to a 41-layer 1/25° HYCOM simulation with realistic tides and atmospheric forcing
  GOAL: -verify that the barotropic improvements are maintained

-diagnose impact on internal tides

- Perform a short global 1/50° 41-layer simulation initialized from 1/25°
  GOAL: quantify the effect of increased resolution everywhere (e.g. the barotropic tides, baroclinic tides, and internal gravity wave spectrum)

The key individuals involved in this research are given below.

-- Maarten Buijsman of the University of Southern Mississippi (USM) is the PI on this research project. In the last five years Buijsman has collaborated with researchers at Naval Research Laboratory (NRL) and University of Michigan (UM) to improve tides in HYCOM. Buijsman has worked on re-tuning the topographic wave drag in HYCOM (*Buijsman et al, 2015*), he has developed tidal energy diagnostics for HYCOM (*Buijsman et al, 2016*), and he has investigated the causes of internal tide incoherence near the equator (*Buijsman et al., 2017*). Buijsman works closely with collaborators, listed below, to coordinate the progress of the HYCOM two-way nesting project. For this purpose, weekly conference calls with the collaborators have been established. Buijsman will diagnose the model solutions, write papers, supervise full-time graduate students Victoria Young and Heather McCain, supervise post-docs Chan-Hoo Jeon and Gordon Stephenson, keep track of the milestones, write annual reports, manage the subcontract to Brian Arbic of the University of Michigan, and collaborate with Arbic, Jim Richman of Florida State University, and Jay Shriver and Alan Wallcraft of the Naval Research Laboratory. Buijsman will also act as the liaison between NRL and the PIs of the other NOPP projects and Inner Shelf DRIs and handle their requests for access to HYCOM model data.

--Chan-Hoo Jeon, a South Korean National, was hired in June 2016 as a postdoctoral scholar to implement the OASIS nesting package to allow for HYCOM to HYCOM two-way nesting. Jeon's work is also relevant for the NOPP project "Arctic Shelf and Large Rivers: Seamless Nesting in Global HYCOM".

--Gordon Stephenson was hired in April of 2016 as a postdoctoral scholar. He is performing and analyzing 1/12.5° and 1/25° HYCOM simulations. Stephenson is also involved with setting up and running 2D HYCOM simulations as part of the NOPP project 'Russian Dolls: Nesting a turbulent Large Eddy Simulation within a nonhydrostatic Adaptive Grid Model within a 1/25° HYCOM model' led by A. Scotti.

--Victoria Young started in the fall of 2015 as Buijsman's graduate student at USM. Young has been running the tidal and internal tide energy diagnostics, developed by Buijsman, on the HPC of DOD for existing 1/12.5° simulations performed by Joseph Ansong, Arbic's postdoc. In these simulations the effect of the wave drag strength on the tides and internal tides is scrutinized. Due to personal reasons Young left the university in January of 2016. Her work has been continued by Stephenson**.**

--Heather McCain started in the summer of 2016 at USM. She is funded by an NSF grant to study the evolution of Hybrid Kelvin Edge waves on continental shelves in 1/25° HYCOM. She has been diagnosing the 1/25° HYCOM simulations on the HPC. Her analysis is valuable for improving our understanding of HYCOM's surface and internal tide energetics.

--Brian K. Arbic is a co-PI on this grant. Arbic has worked, and continues to work, with NRL collaborators to understand and improve several aspects of the HYCOM tides simulations, including self-attraction and loading, topographic wave drag, implementation of the ASEnKF SAL (*Ngodock et al. 2016*), examination of the impact of stratification on the barotropic tidal field, and examination of the internal gravity wave continuum in HYCOM (*Müller et al. 2015, Savage et al. 2017a, Savage et al. 2017b*). Arbic and his group members have led several analyses of the HYCOM results as described below. Arbic's subaward for the new grant N00014-15-1-2288 includes funding for two U.S. citizen graduate students, Anna Savage and Conrad Luecke. The grant also supported Arbic's time on two papers written on HYCOM by his former postdocs David Trossman and Patrick Timko (*Trossman et al. 2017, Timko et al. 2017).*

--Joseph Ansong is a postdoc in Arbic's UM group. Ansong has published two papers thus far on analyses of HYCOM; one (*Ansong et al. 2015*) on the impacts of internal wave drag on the internal tide field, and one (*Ansong et al. 2017a*) on model-data comparisons of internal tide energy fluxes. Ansong has two additional papers in preparation, one on parametric subharmonic instability (PSI) in HYCOM (*Ansong et al. 2017b*), and one on internal gravity wave kinetic energy spectrum in HYCOM and the MITgcm (*Ansong et al. 2017c*).

--Anna Savage is a graduate student in the UM Applied Physics Program. Savage is comparing sea surface height frequency spectra in HYCOM versus tide gauges and moored instruments, and is comparing the widths of tidal peaks in sea surface height frequency spectra in tide gauges versus simulations with and without eddies as an alternative method for quantifying internal tide non-stationarity. She has performed three analyses of relevance for the planned wide-swath satellite altimeter mission (SWOT; Surface Water Ocean Topography). She has begun using HYCOM and the MITgcm to test tidal aliasing issues for SWOT. She has computed frequency-wavenumber spectra of sea surface height, in order to determine whether high-frequency internal waves versus lower frequency motions dominate particular portions of the wavenumber spectrum (Savage et al. 2017b). Finally, Savage has also constructed global maps of the sea surface height signatures of the internal gravity wave continuum (Savage et al, 2017a).

--Conrad Luecke, graduate student in the UM Department of Earth and Environmental Sciences: Luecke is working with Arbic and NRL collaborators to compare both low-frequency (*Luecke et al. 2017*) and high-frequency temperature variance and kinetic energy in HYCOM and in MITgcm with those in historical temperature records. After Luecke has published these model/data comparisons, he will construct global three-dimensional maps of potential and kinetic energy in different frequency bands (geostrophic/mesoscale, near-inertial, and tidal) from the HYCOM and MITgcm simulations. Luecke will also compare slopes, and non-stationarity, of the spectra of high-frequency kinetic energy and temperature variance (e.g., in the internal gravity wave band) in the models with those in historical current meter and temperature records, respectively.

-- Jay Shriver has also contributed to most of the projects described in this document. He is currently running the new HYCOM 1/25° and 1/75° tidal simulations, and has led global comparisons of HYCOM to the TOPEX/POSEIDON-Jason along-track altimetric tidal analysis of Richard Ray, and an examination of the temporal stationarity of internal tides, both topics of great interest to NASA.

--Alan Wallcraft has collaborated with Arbic to insert tides into the HYCOM code. Wallcraft has participated in most of the projects described in this document. He has prepared the 1/75° one-layer HYCOM simulations. Wallcraft and Shriver are assisting Jeon with the implementation of the OASIS package for the two-way nesting. The two-way nesting capabilities will also be applied in the "Arctic

Shelf and Large Rivers: Seamless Nesting in Global HYCOM" project, led by Eric Chassignet with Pat Hogan, Jim Richman, and Alan Wallcraft.

--Jim Richman has been an active contributor to most of the projects described in this document, and took the lead on examining the impact of internal tides on the wavenumber spectra of sea surface height, a subject of great interest to NASA as it prepares for the wide-swath satellite altimeter.

--Luis Zamudio of the Naval Research Laboratory is running some of the new HYCOM tide simulations, and helps with the post processing of the large data sets. He has provided critical assistance to various projects described in this document.

WORK COMPLETED

This project is now just past the beginning of its third year, and since the last reporting cycle we have accomplished new results. In this and the next section we highlight completed tasks and present results for existing HYCOM solutions.

Post-doctoral scholar Jeon has worked for more than one year on setting up two-way nesting in HYCOM using the OASIS coupler package. In collaboration with Wallcraft and Shriver, Jeon has successfully tested the coupler for one-way and two-way nested barotropic HYCOM simulations for parent and nested grids with the same resolution of 1/25°. Currently, Jeon is performing nesting simulations in which a child grid with a resolution of 1/75° is nested in global and regional parent grids with a resolution of 1/25°. These results are also summarized in a journal article.

Shriver, Wallcraft and Buijsman have updated the global high resolution bathymetry used in barotropic 1/75° HYCOM and performed new simulations. The bathymetry update comprises a more accurate Southern Ocean bathymetry from BEDMAP2. New 1/25° and 1/75° HYCOM simulations have been performed to tune the wave drag. The high resolution bathymetry will be used in the regional 1/75° domains that are nested in the coarser 1/25° global model.

To provide boundary conditions for our own two-way nesting projects, and our NOPP and DRI collaborators, Shriver and NRL collaborators have been performing global 3D simulations of the non-assimilative and assimilative 1/25° models. Previously we have run an initial data assimilative simulation spanning November 2013 to August 2014. During the past year a non-assimilative simulation was run from November 2013 to the end of 2014. The model data that is stored are hourly SSH and barotropic velocity fields, daily-mean 3D fields, and monthly startup files. For the non-assimilative simulation, hourly 3D fields have been stored for September 2014. We have begun a new data assimilative run that will span the period December 2015 – present. We are planning to run a non-assimilative twin of this experiment which will help us address the question of internal tide predictability. An analysis by Buijsman highlighted thermobaric instability issues that we are presently working to resolve. We also collaborated with scientists at several institutions (including WHOI, Scripps, U. Washington, U. of Hawaii) who assisted in vetting the non-assimilative 1/25° HYCOM with tides simulation through two refereed journal submissions that utilize these results. Their work highlighted code/script bugs that were fixed.

In the last year we have published 6 journal refereed articles and submitted 4 journal articles.

RESULTS

A nesting framework using OASIS3-MCT (*Valcke et al., 2015*) has been implemented by Post-doctoral scholar Jeon to improve global barotropic tides in the HYCOM global ocean circulation model. The two-way nesting framework is applied to realistic regional and global modeling cases. The geographical domains of the child and the parent components are shown in **Figure 1**. Both cases consist of a parent and a child domain. The Hudson Strait and vicinity (HUD) is the child domain. The parent domain is a regional grid (ARC) and a global grid (GLB). In the regional case, the parent domain includes the Arctic Ocean and the North Atlantic Ocean. The resolution of the child domain (1/75°) is three times as fine as that of the parent domain (1/25°). In these simulations the bathymetry of the child grid is interpolated from the 1/25° parent grid. Hence, the child grid does not include the most accurate bathymetry. Jeon will include a high resolution bathymetry in future simulations. The child and the parent domains are forced by five leading tidal constituents (M_2, S_2, N_2, K_1, and O_1) and the mean sea level pressure (MSLP). The sea surface heights are stored every hour for harmonic analysis during a 28-day simulation.

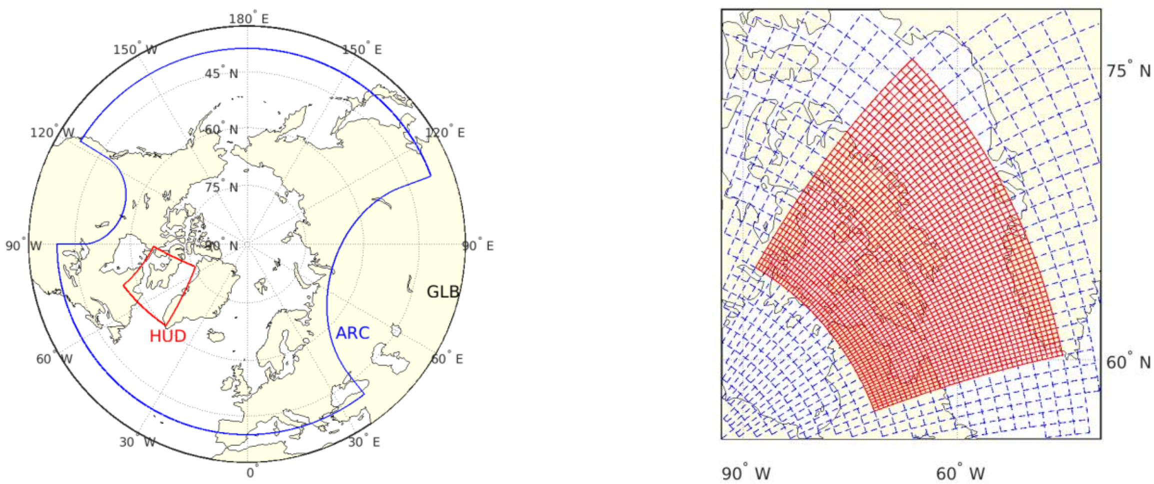

Figure 1. Geographical domains and grid resolution. The child domain (HUD), the parent domain for a regional case (ARC), and the parent domain for a global case (GLB)

In the regional case, the child domain receives forcing from the parent domain through its lateral boundary. The parent domain is forced with offline tidal forcing extracted from the global model. **Figure 2** presents the sea surface height (SSH) root-mean-square errors (RMSE) between TPXO8-atlas on the one hand and the reference solution on the parent grid and the two-way nesting solution on the other. The reference solution does not include two-way nesting. The reduction of RMSE due to two-way nesting in **Figure 2** is calculated by subtracting the results of two-way nesting from the results of the reference parent solution. The red and yellow (blue) zones indicate the RMSE with TPXO8-atlas has been reduced (increased) due two-way nesting. The reduction in RMSE is not limited to the child domain. The effects of the two-way nesting spread beyond the boundaries of the child domain. The two-way nesting causes improvements in the tidal solution on the parent domain, illustrating the non-local or back-effect of the tides.

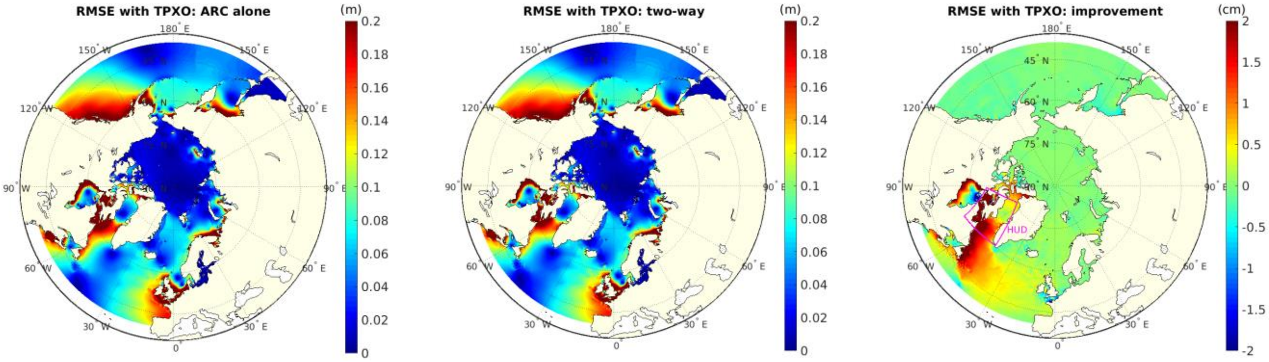

Figure 2. SSH Root-Mean-Square error between TPXO8-atlas on the one hand and the reference solution on the parent grid (a) and the two-way nesting solution (b) on the other, and the RMSE reduction (improvement) due to two-way nesting in the regional case (c). Red color is better tides and blue color is worse tides.

For the global case, the child domain is the same as before. **Figure 3** shows the reduction in the RMSE with TPXO8-atlas due to two-way nesting. Most of the improvement is observed in the North Atlantic Ocean where the high-resolution child domain is located. Especially, the area around the European Shelf in the North Atlantic Ocean shows a remarkable improvement compared to the regional case in **Figure 2**, even though the tides in the English Channel have become less accurate. The other ocean basins do not show any large improvements.

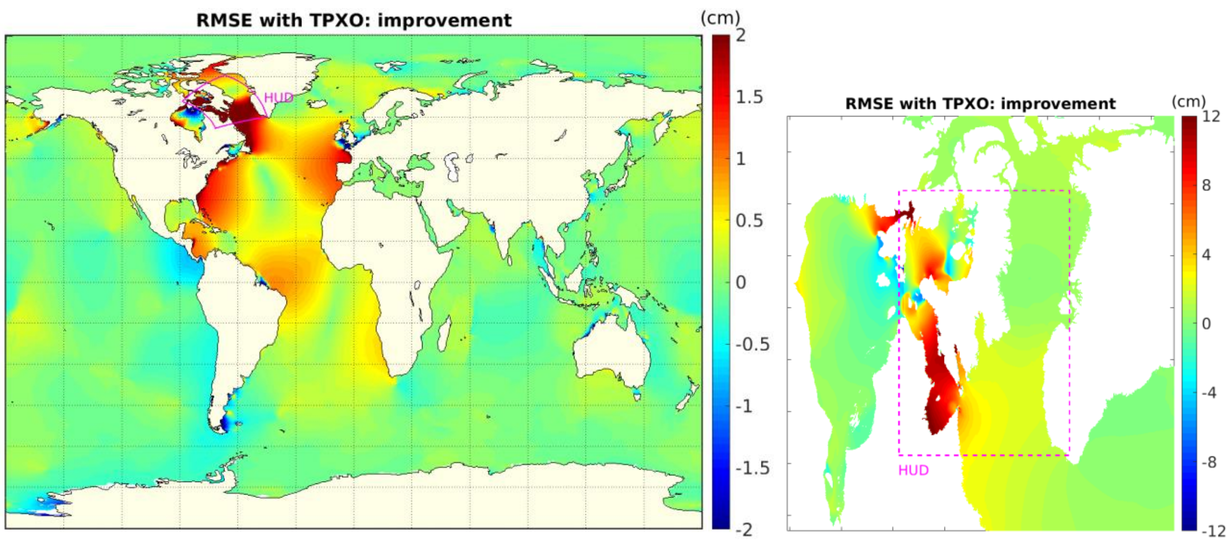

Figure 3. Reduction of RMSE due to two-way nesting on the parent (GLB) domain and its zoom-in around the child domain (HUD). The reduction of RMSE due to two-way nesting is calculated by subtracting the results of two-way nesting from the results of the reference parent solution. Red is better tides and blue is worse tides.

Table 1 presents the SSH RMSE with TPXO8-atlas averaged over ocean area (RMS_{avg}). The second and the third columns denote RMS_{avg} computed for the child area (HUD_{GLB}) and the ARC area (ARC_{GLB}) on the global parent domain (GLB). RMS_{avg} over the global parent domain is shown in the fourth column (GLB). RMS_{avg} is computed over water depths greater than 1000m and latitudes equatorward of 66° and is in the fifth column (GLB_{66}). RMS_{avg} is reduced due to two-way nesting for all 4 areas. The magnitude of the reduction is higher near the child domain.

We have shown that local and remote tides can be improved with a higher resolution nest in a regional and a global model. In future work, Jeon will include a more accurate child bathymetry and apply two-way nesting to a larger child grid and to multiple child grids to further reduce the RMSE.

Table 1. SSH Root-Mean-Square error averaged over the domain

	HUD_{GLB}	**ARC_{GLB}**	**GLB**	**GLB_{66}**
GLB alone	29.76 cm	9.53 cm	6.43 cm	4.12 cm
Two-way nesting	26.90 cm	9.06 cm	6.34 cm	4.01 cm

Similar to the 1/12.5° tuning experiments (*Buijsman et al, 2015*), Buijsman and NRL collaborators Shriver and Wallcraft have performed and analyzed tuning experiments with the global barotropic 1/25° and 1/75° tidal simulations. These simulations are performed for 5 tidal constituents, a high resolution GEBCO bathymetry, and a spatially varying scalar self-attraction and loading term. The drag scale, the tuning parameter for wave drag in HYCOM, is varied from 0.225 to 0.450, and a value of 0.3 yields the lowest Root-Mean Square Error of 2.9 cm for the M_2 tidal constituent (**Figure 4**). **Figure 4** shows the tuning curves as a function of RMS error and wave drag dissipation in deep water and the bottom drag dissipation in shallow water. On the shallow shelves the bottom drag dissipation is larger when the total velocity based on all tidal constituents is applied, whereas it is lower when the dissipation is computed from the sum of the individual constituents. Hence, we crudely correct the M_2 dissipation in shallow water (blue and red dashed lines) to account for this nonlinear coupling, bringing the results in closer agreement with the M_2 dissipation estimated from TPXO8-atlas. The RMS errors of the 1/12.5° and 1/25° tuning experiments, as represented by the black dashed and red curves in **Figure 4**, are significantly higher than the 1/75° simulations. This illustrates that a higher model resolution and a more accurate representation of the coastal geometry yields more accurate tides. The question that we aim to address is whether the two-way nesting of resonant coastal areas, such as the Hudson Strait, can result in similar improvements.

The 1/75° simulations using GEBCO bathymetry do not have a correct representation of the bathymetry in the Southern Ocean. Shriver, Wallcraft, and Buijsman updated the Southern Ocean bathymetry with the more accurate BEDMAP2 bathymetry (http://www.scar.org/data-products/bedmap). BEDMAP2 bathymetry represents the water depths under the ice shelfs more accurately than GEBCO. However, this improvement did not lower, but yielded the same RMS error as the previous simulation with a drag scale of 0.375 and without the BEDMAP2 update (magenta circle in **Figure 4**).

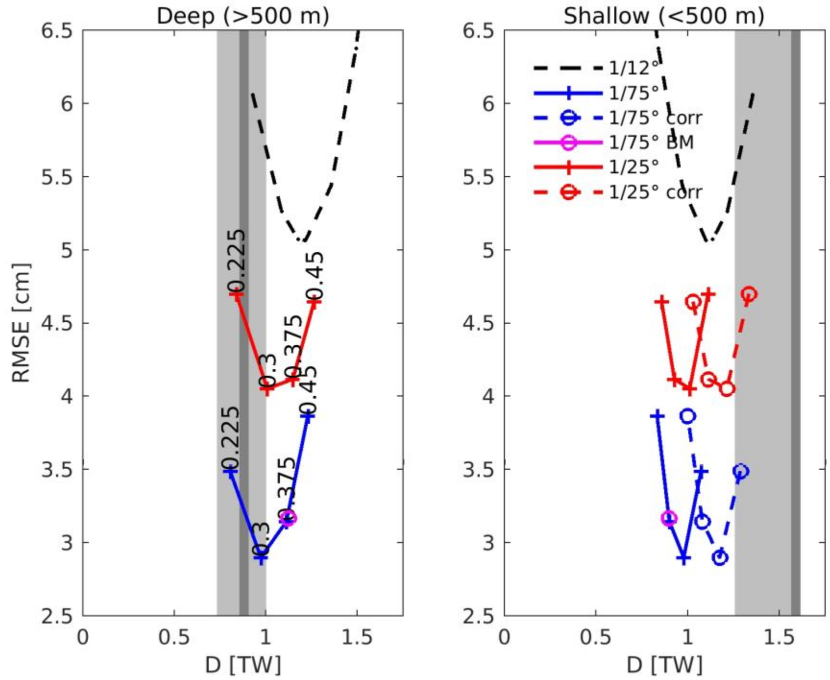

Figure 4. The deep water (H>500 m) and shallow water (H<500 m) HYCOM dissipation rates vs. RMS error as a function of drag scale for the 1/12.5° (black), 1/25° (red), and 1/75° (blue) simulations. The '1/75° BM' simulation with the BEDMAP2 Southern Ocean bathymetry is marked the magenta circle. The RMS error is computed between HYCOM and TPXO8-atlas M_2 sea surface heights for H>1000 m and equatorward of 66°. The range of the TPXO dissipation rates is marked by the light gray box and TPXO8-atlas (the most recent TPXO inverse model) by the dark gray line. A minimal RMSE of 2.9 cm is obtained for a drag scale of 0.3.

Realistically forced global models also give insight into how internal tides interact with mesoscale circulation such as jets and eddies. At generation, internal tides are coherent with the local barotropic forcing, but as the low mode waves propagate through an eddying ocean, their phases become incoherent with the forcing. While satellite altimetry can only map the coherent part of the internal tide, HYCOM captures both the coherent and incoherent parts. Hence, HYCOM can be used to distinguish between tidal and mesoscale variability in the altimetry data from the upcoming SWOT mission. One of the regions in the world where internal tides are strongly incoherent is the Equatorial Pacific. In HYCOM 1/12.5° simulations, Buijsman has found that the jets in the equatorial Pacific Ocean yield a strong loss of phase coherence in semidiurnal internal tides that propagate equatorward from the French Polynesian islands and Hawaii (**Figure 5**). The loss of phase coherence is attributed to the time variability in the advection by the sheared zonal jet velocities. For time scales longer than a year the coherent energy flux approaches zero values at the equator, while the total flux, comprising the sum of the coherent and incoherent fluxes, remains non-zero. The 1/12.5° model simulation suggests that low-frequency jets do not noticeably enhance the dissipation of the internal tide, but merely decohere and scatter it. Thus, the model results suggest that the apparent demise of coherent internal tides seen in satellite altimetry maps may be due to incoherence rather than dissipation. These results have been summarized in a paper that has been published in the Journal of Geophysical Research (*Buijsman et al., 2017*).

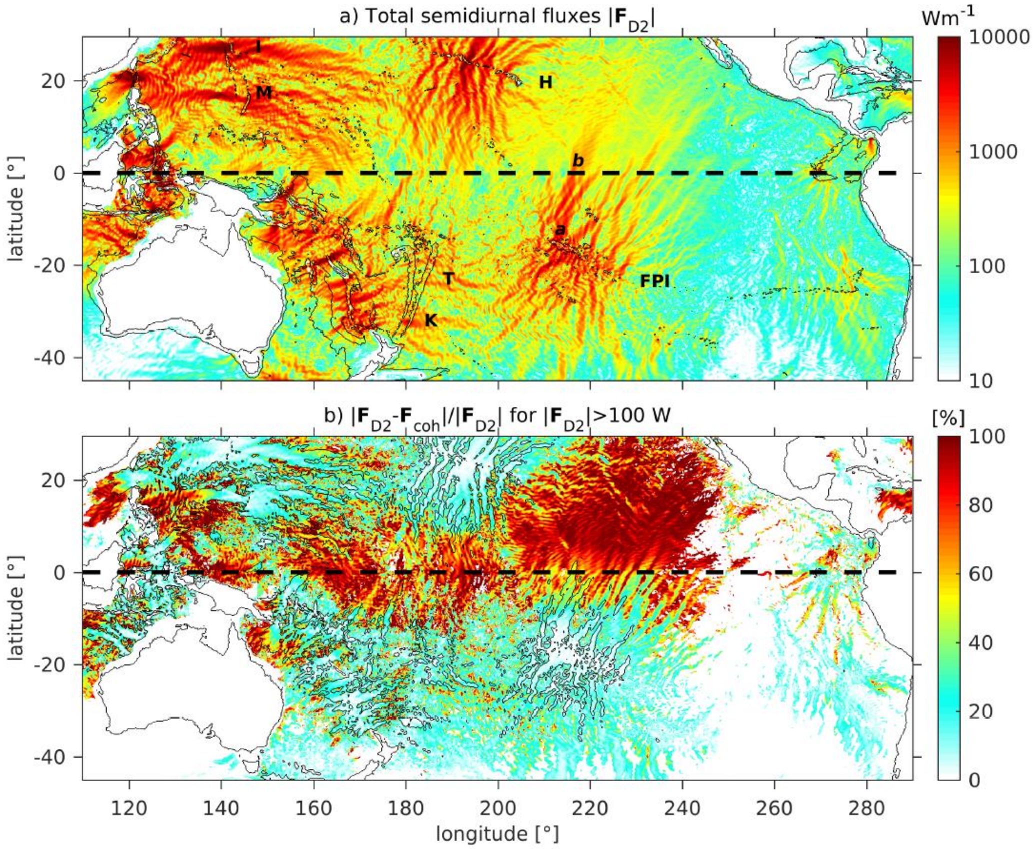

Figure 5. (a) The magnitude of the annual-mean semidiurnal total energy fluxes in the equatorial Pacific from HYCOM. Bathymetry is contoured at 0 and -2000 m. Hawaii is abbreviated with H, the French Polynesian Islands with FPI, Tonga with T, the Kermadec Islands with K, the Izu Ogasawara Ridge with I, and the Mariana Islands with M. (b) The percentage of the sum of the annual-mean incoherent fluxes to the semidiurnal total fluxes. The black contours mark 1000 W m^{-1} of the total fluxes. Bathymetry is contoured at 0 m. In both subplots, the equator is marked by the dashed black line. While the internal tides can be seen to cross the equator in (a) they become phase incoherent (i.e., less predictable) when they do in (b).

To further expand our understanding of how the internal tide generation at seamounts is affected by remotely generated internal tides, Buijsman has collaborated with L. Zhang, H. Swinney, and student E. Comino. In this project Buijsman has supervised Comino in performing idealized MITgcm simulations of internal tide generation at seamounts. We find that if sea mounts are in close proximity of each other, then they are less effective in converting surface tidal energy to internal tides (a reduction of ~15%; **Figure 6**). These efforts have been published in the Journal of Geophysical Research (*Zhang et al., 2017*).

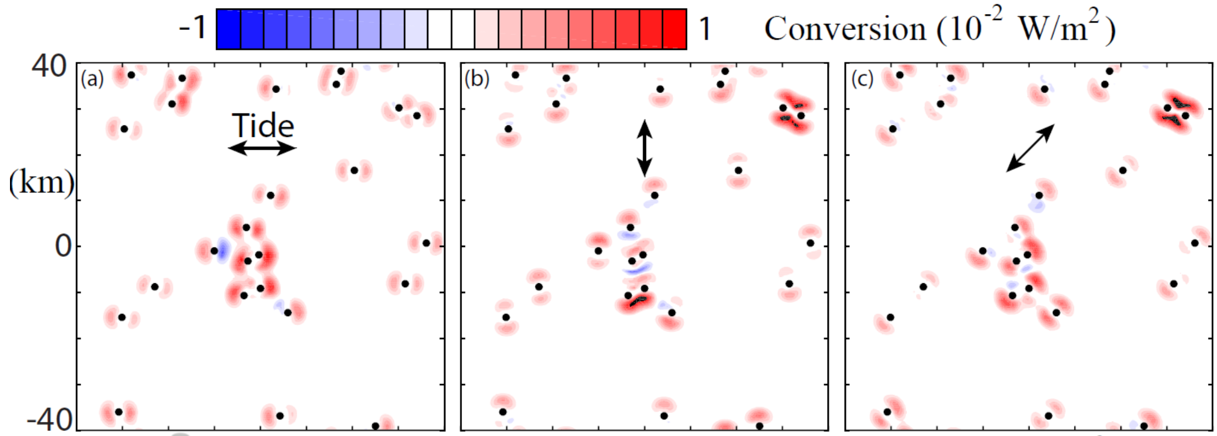

Figure 6. Barotropic to baroclinic energy conversion for three realizations of randomly placed seamounts. Closely placed seamounts undergo destructive interference causing smaller or more negative conversion values (blue).

Post-doctoral scholar Stephenson has worked on the modal decomposition of internal tides in global 1/12.5° and 1/25° simulations in HYCOM. In HYCOM the dissipation of resolved internal wave modes is accounted for by a wave drag term. In 1/12.5° HYCOM, the drag strength is about twice as large as in 1/25° HYCOM. With less damping due to a lower wave drag in 1/25° HYCOM, we expect an increase in internal tide energy as compared to 1/12.5° HYCOM. We will investigate if this is the case. We anticipate that as the model resolution increases, more vertical modes and their nonlinear interactions are resolved in HYCOM. We hypothesize that the increase in nonlinear wave-wave interactions facilitates a better energy cascade, reducing the need for a wave drag acting on the wave modes.

Using output from 1/12.5° and 1/25° HYCOM simulations, Stephenson is computing the i) energetics of the baroclinic tide, ii) barotropic to baroclinic conversion, and iii) mode-topography and mode-mean flow interactions. Of interest is the effect of resolution on the representation of scattering of baroclinic modes at topography and by mesoscale variability, including eddies. The main result of this work has been the development of resolution-independent analysis routines to compute the energy budget terms separately for each baroclinic mode. The broader objective of this exercise is to quantify the effects of model resolution on the baroclinic tide, to improve internal wave parameterizations, and to increase the accuracy of the modelled baroclinic tides.

Global maps of modal kinetic energy for the lowest two baroclinic modes in **Figure 7** illustrate some of the features of baroclinic modes. Strong beams of internal tide energy radiate from generation sites near steep topography, such as the Hawaiian island chain and the Aleutian archipelago. The spatial scale of the tidal beam features, such as distance between peaks and minima in kinetic energy along a beam, shrinks with increasing mode number, as does the length of tidal beams. While mode-1 energy crosses the Pacific basin (**Figure 7** top), the energy in mode 2 (**Figure 7** bottom) decays over shorter O(500-1000 km) spatial scales. Global integrals of the modal baroclinic kinetic energies yield a total of 60.8 PJ, in agreement with other estimates of the total coherent kinetic energy in the M_2 baroclinic tide, and attribute 40.0 PJ (65.8%) to the mode 1 baroclinic tide, 13.7 PJ (22.5%) to mode 2, 4.1 (6.7%) PJ to mode 3, 2.0 PJ (3.3%) to mode 4, and 0.9 PJ (1.5%) to mode 5. Similar global calculations for available potential energy, baroclinic energy fluxes, conversion, and dissipation are currently being refined.

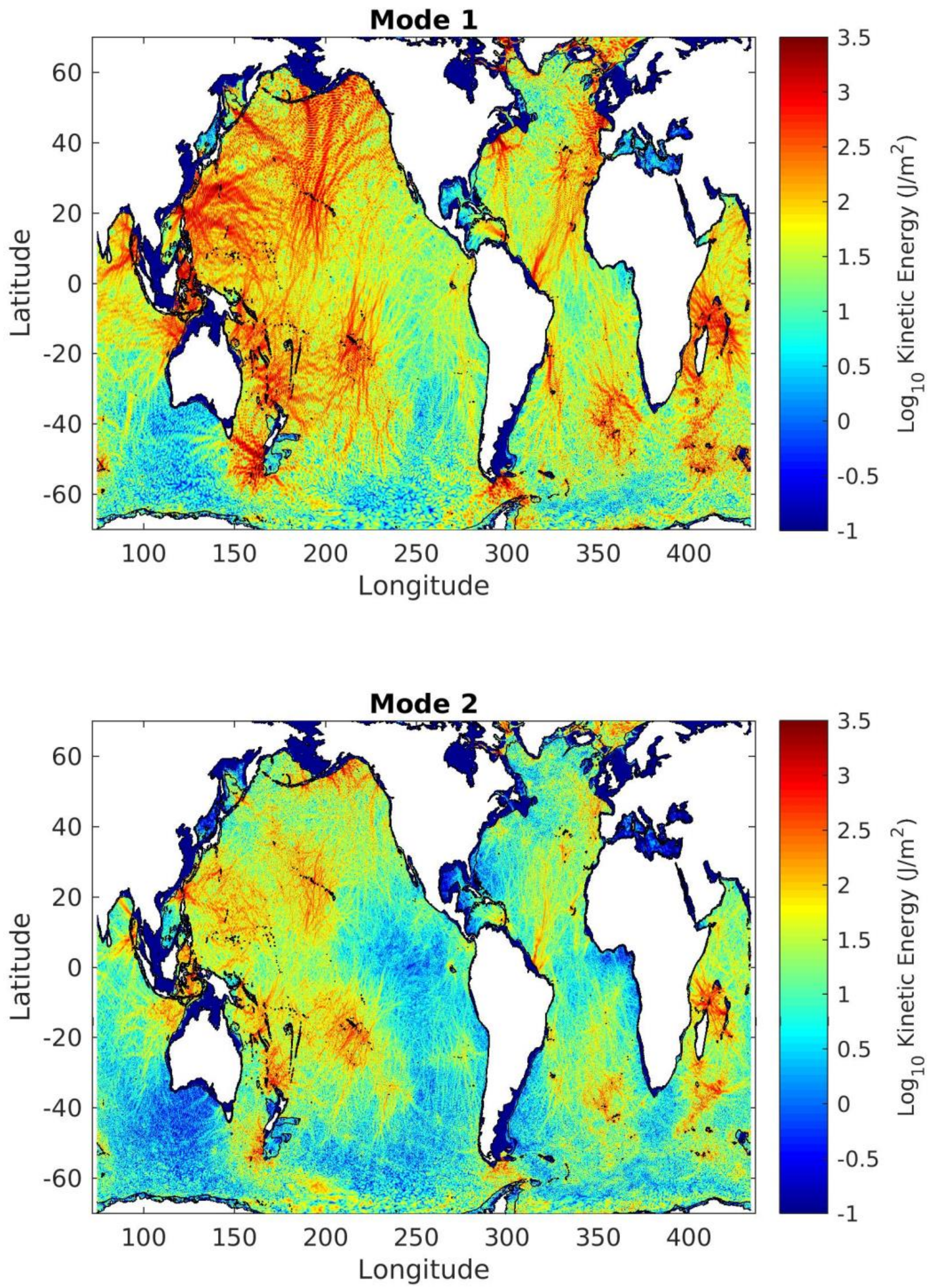

Figure 7. Global maps of the depth-integrated M_2 kinetic energy in baroclinic modes 1 and 2. Low-mode tidal beams propagate hundreds or thousands of kilometers from generation sites at the ocean margin and near island chains.

Student Young has diagnosed 1/12.5° simulations 051 and 052 that have been performed by *Ansong et al (2015)*. NSF-funded student McCain has diagnosed the 1/25° simulation 101. In the following their results are summarized. The aim of this comparison is to determine the effect of different horizontal resolutions on the internal tide energetics in HYCOM.

The 051 simulation has wave drag acting on the total velocities, while 052 has the wave drag acting only on the barotropic velocities. In both cases the wave drag scale is 0.5. Because the drag does not act on the internal waves in 052, the internal tides do not loose energy to the wave drag (see the zero values in the bottom center panel of **Figure 8**). In 051 about 50% of the loss of internal tide energy D_{tot} in deep water (>2000 m) is due to the wave drag D_w (compare bottom with top panels). As a consequence, the absence of wave drag in 052 causes less deep water dissipation ($D_{tot}/C=0.5$) as compared to 051 ($D_{tot}/C=0.6$). This is offset with slightly more shallow water dissipation in 052. This implies that more internal tide energy propagates from deep water into the shallower coastal zones. Following Zhao et al (2016), we applied a plane wave technique to track unidirectional internal tides into the coastal zone. In 051 we find that about 12% of the waves generated in deep water propagates into the coastal zone, while in 052 this is about 20%. Hence, this is in agreement with our findings in **Figure 8**.

The dissipation in the 101 simulation is very similar as in the 051 simulation, albeit with some subtle differences (top panels). The fraction of the energy lost to the wave drag is reduced by 1/3 in the 101 simulation as compared to the 051 simulation (bottom panels). This is in accordance with the reduction in drag scale strength from 0.5 to 0.3. In contrast, the dissipation D_{tot}/C in deep water is not reduced by 1/3 in 101 (top panels). This may imply that the increased horizontal resolution in 101 allows for a better energy cascade to higher modes through wave-wave interaction. This contrasts with Buijsman et al (2016), who argued that the 1/25° simulations would be too energetic, which is not necessarily the case.

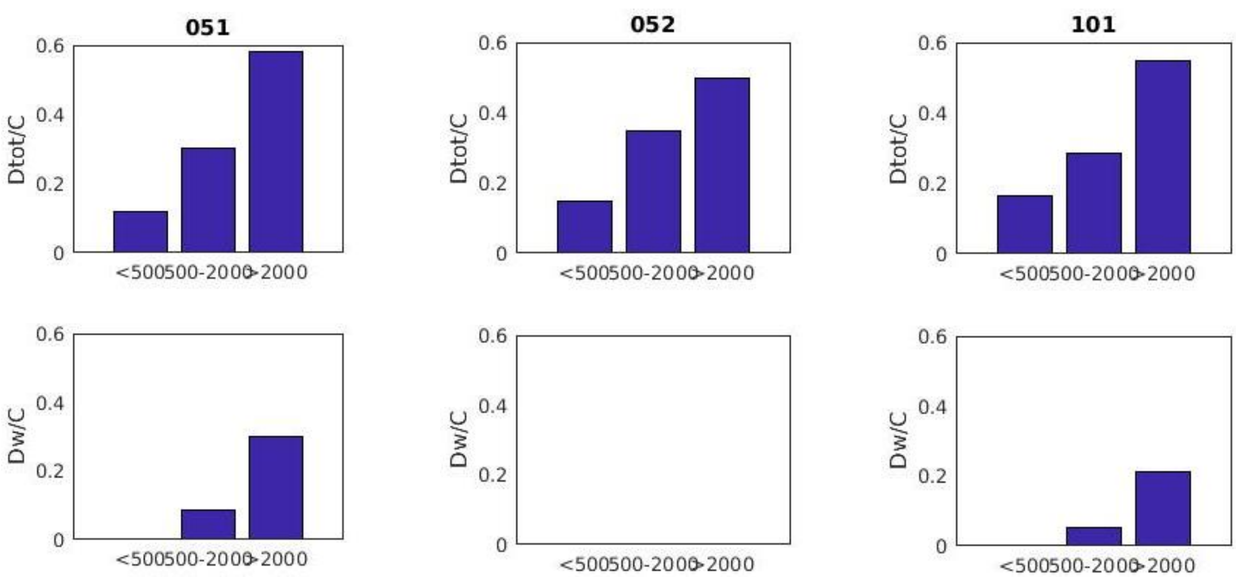

Figure 8. The deep water dissipation (top) and wave drag dissipation (bottom) as a fraction of conversion for two 1/12.5° simulations 051 and 052 and the 1/25° simulation 101. The dissipation is binned in three bottom depth ranges: <500 m, 500-2000 m, and >2000 m. D_{tot} is the total

internal tide dissipation, C is the barotropic to baroclinic conversion, and D_w is the internal tide energy lost to the wave drag. Values are normalized by the globally integrated conversion C.

Buijsman and Arbic have also contributed their HYCOM analysis to the NSF funded Climate Process Team on internal-wave driven mixing. They have contributed maps of internal-wave dissipation as computed with HYCOM. Their results have been incorporated in an article that has been published in the journal of the American Meteorological Society (*McKinnon et al., 2017*).

The work of Arbic's group has focused on internal tides and the internal gravity wave continuum. Postdoc Joseph Ansong showed that the mean and variability of internal tide energy fluxes in HYCOM is comparable to that in current meter observations (*Ansong et al. 2017a*). The large variability seen in observed fluxes implies that the fluxes inferred from short current meter records have large error bars. Ansong's next paper (*Ansong et al. 2017b*) demonstrates that parametric subharmonic instability (PSI) does take place at the predicted critical latitudes in HYCOM, and that the PSI sink of tidal energy is an order of magnitude larger in 1/25º HYCOM than in 1/12º HYCOM, though the sink is still small relative to the total global tidal dissipation. *Ansong et al. 2017c*, the final paper that Ansong is writing before he leaves Michigan for a faculty position in Ghana, demonstrates that both HYCOM and recent MITgcm simulations that are also simultaneously forced by atmospheric fields and the astronomical tidal potential have a realistic internal gravity wave kinetic energy spectrum, that lies closer to observations as model resolution increases. **Figure 9** displays vertical wavenumber-frequency spectra from a McLane profiler and from nearest neighbor gridpoints taken from the 1/48º MITgcm and 1/25º HYCOM simulations. The figure demonstrates that the models have nearly equal amounts of upward- and downward-propagating motions, as in the observations, though the energy falls off more rapidly with high vertical wavenumber in the models. **Figure 10**, taken from *Savage et al. 2017b*, demonstrates that the frequency spectra of dynamic height in 1/48º MITgcm and 1/25º HYCOM simulations compares reasonably well with frequency spectra computed from 9 McLane Profilers throughout the Pacific Ocean.

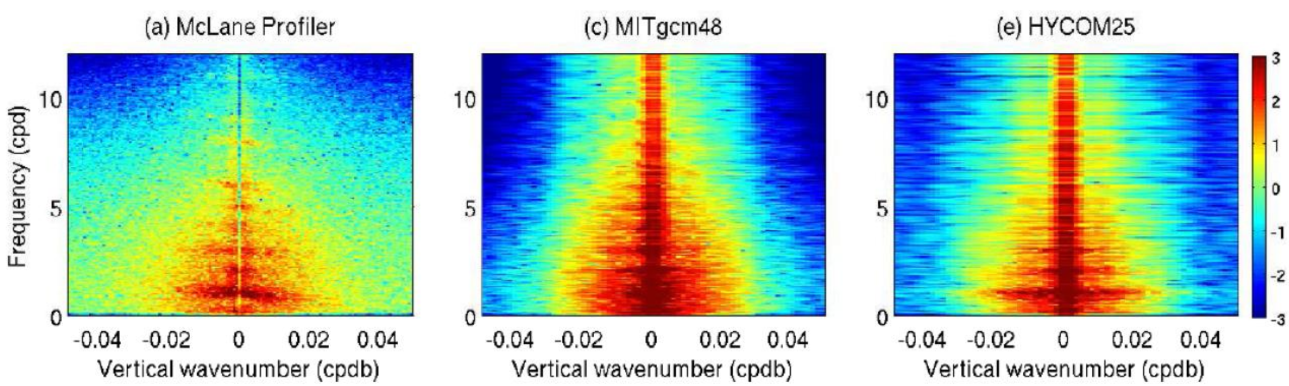

Figure 9. Frequency-vertical wavenumber spectral density [$\log_{10}$ (cm/s)^2 / [(cycle per decibar * cycle per day)] for McLane profiler at 121.0ºE, 19.3ºN and nearest neighbor gridpoints of 1/48º MITgcm and 1/25º HYCOM simulations.

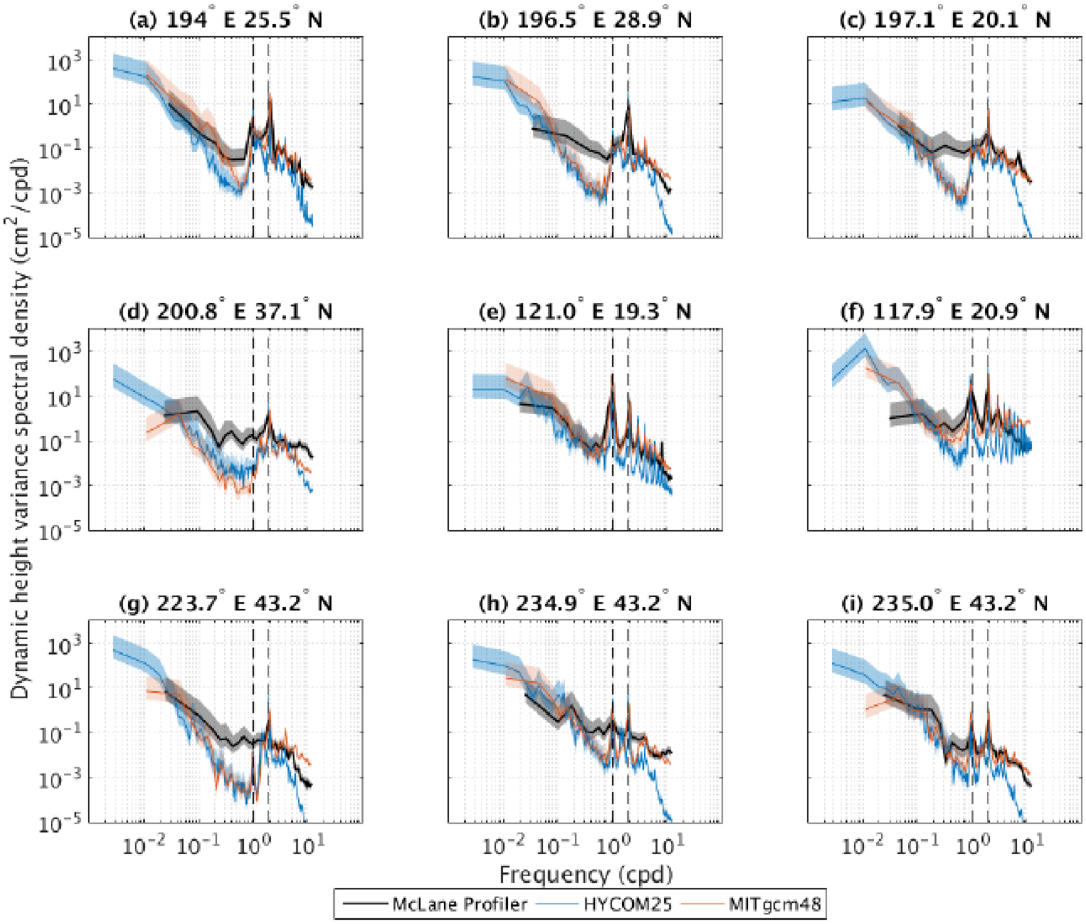

Figure 10. Dynamic height frequency spectral densities from McLane profilers and nearest neighbor 1/25º HYCOM and 1/48º MITgcm gridpoints. The dashed vertical lines denote K1 diurnal and M_2 semidiurnal tidal frequencies. The shaded regions are the 95% confidence intervals, which account only for random error in spectral density calculations.

Finally, **Figure 11** displays global maps of frequency-band-integrated steric sea surface from 1/25º HYCOM (*Savage et al. 2017a*). The maps in Figure 15 display the non-stationary semidiurnal tides, and the supertidal motions; the latter are dominated by internal gravity waves, and the figure is the first to show global maps of such motions. The work in Savage's two 2017 papers is of direct relevance to the planned upcoming SWOT mission.

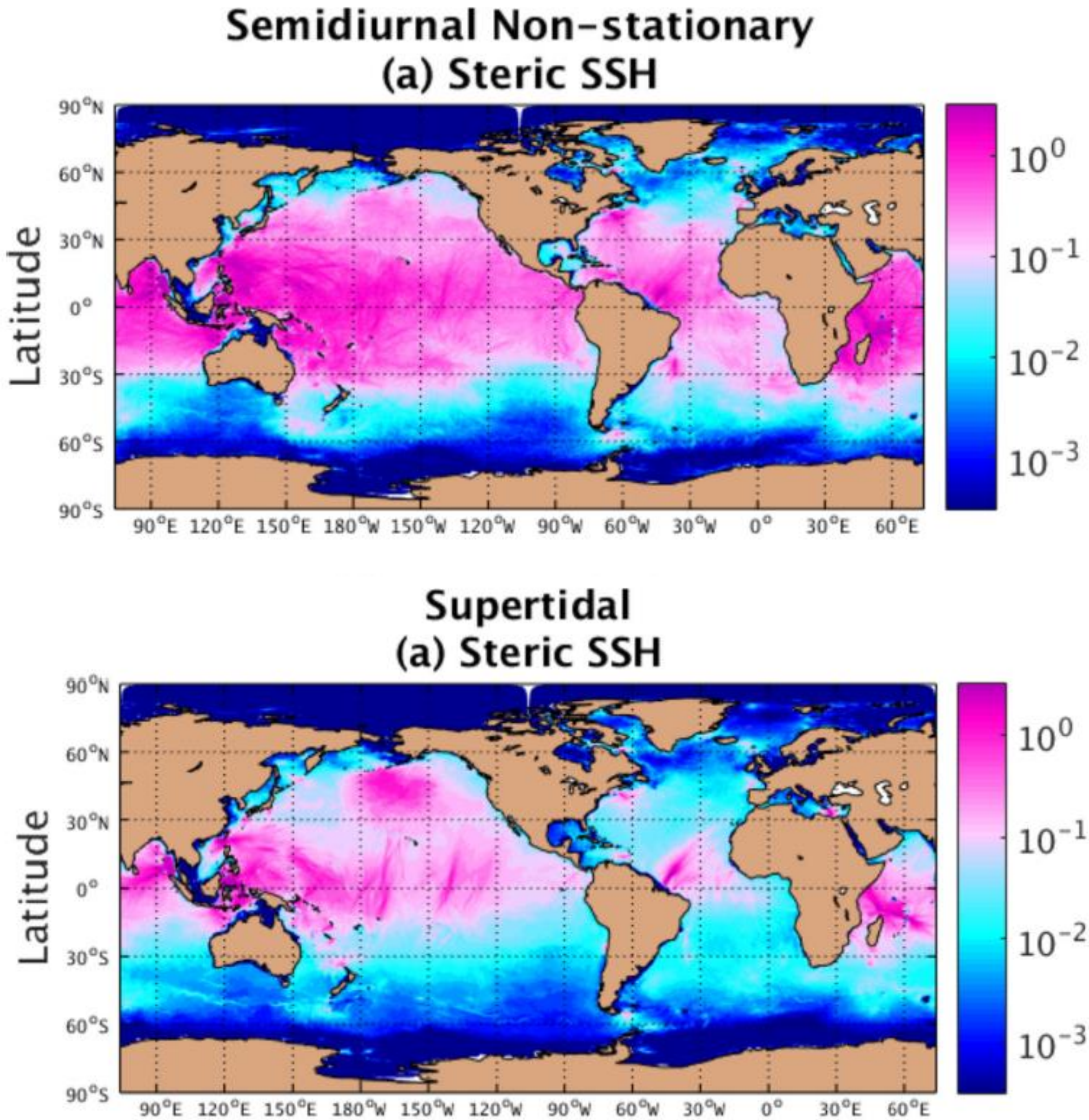

Figure 11. (Top) Global SSH variance (cm^2) from 1/25º HYCOM in the semidiurnal band (frequencies 1.86–2.05 cpd) after stationary tides have been removed via harmonic analysis. The 95% confidence intervals range from 92% to 109% of shown value. (Bottom) As in top but for the supertidal band (2.06-12 cpd). The 95% confidence intervals range from 98% to 101% of shown value.

IMPACT/APPLICATIONS

A successful implementation of the two-way nesting technique in HYCOM is highly beneficial for operational purposes. This technique has a significant advantage over the current one-way nesting approach with significantly lower cost than increasing the model resolution everywhere. The technique can be applied to areas where tidal resonance requires an accurate and detailed representation of the coastal geometry. In addition, the technique can be applied to regions that require a higher resolution of the ocean currents and stratification for U.S. Navy operational purposes.

RELATED PROJECTS

A related project that also studies two-way nesting with OASIS is the NOPP project "Arctic Shelf and Large Rivers: Seamless Nesting in Global HYCOM" led by Eric Chassignet with Pat Hogan, Jim Richman, and Alan Wallcraft. The nesting capabilities developed by postdoc Jeon in the project described here can also be utilized for the HYCOM Arctic rivers project.

Moreover, we are collaborating with NOPP and Inner Shelf DRI scientists to facilitate the access to HYCOM model data. Currently we have received such requests from Pierre F.J Lermusiaux and Brian Powell (NOPP), Falk Feddersen, Nirnimesh Kumar, Ata Suanda, James McWilliams (Innershelf RI).

Arbic, Buijsman, Richman, Shriver, and one other NRL scientist (Hans Ngodock), with Arbic as lead PI, leveraged the work done in HYCOM tides simulations to a position on the Science Team for the NASA/French space agency SWOT) mission. Our HYCOM work featured very prominently in the first meeting of the Science Team, held in June 2016, and Arbic was named co-chair of the High-Resolution Ocean Modeling Working Group for the SWOT Science Team. In addition, Arbic, Buijsman, Ngodock, Shriver, Richman, and Innocent Souopgui of USM have been granted a position on the NASA Ocean Surface Topography Science Team, also based upon their work with tides in HYCOM.

Potential contribution to storage resources: Backed by a letter of support from NRL, Arbic is a "stakeholder" in a new $4.9M NSF Division of Advanced Cyberinfrastructure grant awarded to PI Shawn McKee at the University of Michigan. McKee's project (http://www.nsf.gov/awardsearch/showAward?AWD_ID=1541335&HistoricalAwards=false) is one of 3 such grants awarded around the US, and aims to improve the way in which large datasets are shared between institutions. McKee's grant is targeted mostly at sharing data between 3 research institutions within the state of Michigan, but Arbic's role is to use McKee's infrastructure as a testbed for sharing HYCOM data on a large system with no access restrictions. There is potential for hundreds of TB of HYCOM output to be stored on this system, which could be useful for investigators of the NOPP project N00014-15-1-2288, and/or for other scientists around the world who are interested in our HYCOM tides simulations but who do not have accounts on DoD HPC machines. Already we have used the UM system to provide data for collaborators in Germany as well as to two different Inner Shelf DRI modeling groups (Nirnimesh Kumar of University of Washington and Jim McWilliams of UCLA).

REFERENCES

(all project-related publications in published and submitted between June 2016 and June 2017 are in bold)

Ansong, J. K., B. K. Arbic, M. C. Buijsman, J. G. Richman, J. F. Shriver, and A. J. Wallcraft (2015). Indirect evidence for substantial damping of low-mode internal tides in the open ocean, J. Geophys. Res. Oceans, 120, doi:10.1002/2015JC010998.

Ansong, J. K., B. K. Arbic, M. H. Alford, M. C. Buijsman, J. F. Shriver, Z. Zhao, J. G. Richman, H. L. Simmons, P. G. Timko, A. J. Wallcraft, and L. Zamudio (2017). Semidiurnal internal tide energy fluxes and their variability in a Global Ocean Model and moored observations, J. Geophys. Res. Oceans, 122, doi:10.1002/2016JC012184.

Ansong, J.K., B.K. Arbic, H.L. Simmons, M.H. Alford, M.C. Buijsman, P.G. Timko, E.J. Metzger, J.G. Richman, J.F. Shriver, and A.J. Wallcraft (2017b), Geographical distribution of diurnal and semidiurnal parametric subharmonic instability in a global ocean model, in revision for second review.

Ansong, J.K., B.K. Arbic, M.H. Alford, A.C. Savage, D. Menemenlis, A.K. O'Rourke, J.G. Richman, M.C. Buijsman, J.F. Shirver, A.J. Wallcraft, and L. Zamudio (2017c). Internal gravity wave kinetic energy spectra in global ocean models and observations, in preparation.

Arbic, B.K., S.T. Garner, R.W. Hallberg, and H. L. Simmons (2004). The accuracy of surface elevations in forward global barotropic and baroclinic tide models. Deep Sea Res. II 51, 3069–3101. doi:10.1016/j.dsr2.2004.09.014.

Buijsman, M.C., B.K. Arbic, J.A.M. Green, R.W. Helber, J.G. Richman, J.F. Shriver, P.G. Timko, and A. Wallcraft (2015), Optimizing internal wave drag in a forward barotropic model with semidiurnal tides. Ocean Modell., 85, 42-55

Buijsman, M.C., J. K. Ansong, B.K. Arbic, J.G. Richman, J.F. Shriver, P.G. Timko, A.J. Wallcraft, C.B. Whalen, Z. Zhao (2016). Impact of internal wave drag on the semidiurnal energy balance in a global ocean circulation model. J. Phys. Oceanogr., 46, 1399-1419.

Buijsman, M. C., B. K. Arbic, J. G. Richman, J. F. Shriver, A. J. Wallcraft, and L. Zamudio (2017). Semidiurnal internal tide incoherence in the equatorial Pacific, J. Geophys. Res. Oceans, 122, doi:10.1002/2016JC012590.

Falahat S., J. Nycander, F. Roquet, and M. Zarroug (2014). Global Calculation of Tidal Energy Conversion into Vertical Normal Modes. J. Phys. Oceanogr., 44, 3225-3244.

Jayne, S. R. and L. C. St. Laurent (2001). Parameterizing tidal dissipation over rough topography. Geophys. Res. Lett., 28, 811-814, doi:10.1029/2000GL012044.

Luecke, C.A., B.K. Arbic, S.L. Bassette, J.G. Richman, J.F. Shriver, M.H. Alford, O.M.. Smedstad, P.G. Timko, D.S. Trossman, and A.J. Wallcraft (2017). The global mesoscale eddy available potential energy field in models and observations, in second review.

MacKinnon, J.A., M.H. Alford, J.K. Ansong, B.K. Arbic, A. Barna, B.P. Briegleb, F.O. Bryan, M.C. Buijsman, E.P. Chassignet, G. Danabasoglu, S. Diggs, S.M. Griffies, R.W. Hallberg, S.R. Jayne, M. Jochum, J.M. Klymak, E. Kunze, W.G. Large, S. Legg, B. Mater, A.V. Melet, L.M. Merchant, R. Musgrave, J.D. Nash, N.J. Norton, A. Pickering, R. Pinkel, K. Polzin, H.L. Simmons, L.C. St. Laurent, O.M. Sun, D.S. Trossman, A.F. Waterhouse, C.B. Whalen, and Z. Zhao (2017). Climate Process Team on internal-wave driven ocean mixing. Bull. Amer. Meteor. Soc., 0, doi: 10.1175/BAMS-D-16-0030.1

Müller, M., B.K. Arbic, J.G. Richman, J.F. Shriver, E.L. Kunze, R.B. Scott, A.J. Wallcraft, and L. Zamudio (2015). Toward an internal gravity wave spectrum in global ocean models. Geophysical Research Letters, 42, 3474-3481, doi:10.1002/2015GL063365.

Ngodock, H.E., I Souopgui, A.J. Wallcraft, J.G. Richman, J.F. Shriver, and B.K. Arbic (2016). On improving the accuracy of the M2 barotropic tides embedded in a high-resolution global ocean circulation model. Ocean Modelling, 97, 16-26, doi:10.1016/j.ocemod.2015.10.011.

Savage, A.C., B.K. Arbic, J.G. Richman, J.F. Shriver, M.H. Alford, M.C. Buijsman, J.T. Farrar, H. Sharma, G. Voet, A.J. Wallcraft, and L. Zamudio (2016). Frequency content of sea surface

height variability from internal gravity waves to mesoscale eddies, J. Geophys. Res. Oceans, 122, 2519–2538, doi:10.1002/2016JC012331.

Savage, A.C., B.K. Arbic, M.H. Alford, J.K. Ansong, , J.T. Farrar, D. Menemenlis, A.K. O'Rourke, J.G. Richman, J.F. Shriver, G. Voet, A.J. Wallcraft, and L. Zamudio (2017b). Spectral decomposition of internal gravity wave sea surface height in global models, J. Geophys. Res. Oceans, in revision.

Timko, P.G., P. Hyder, B.K. Arbic, J.G. Richman, L. Zamudio, E. O'Dea, and A.J. Wallcraft (2017). Tidal mixing fronts in a global ocean model, in review.

Trossman, D.S., B.K. Arbic, D.N Straub, J.G. Richman, E.P. Chassignet, A.J. Wallcraft, and X. Xu (2017). The role of rough topography in mediating impacts of bottom drag in eddying ocean circulation models, J. Phys. Oceanogr., doi:10.1175/JPO-D-16-0229.1

Valcke, S., T. Craig, and L. Coquart (2015), 'OASIS3-MCT User Guide', CERFACS/CNRS SUC URA No 1875, CERFACS TR/CMGC/15/38.

Zhang, L., M. C. Buijsman, E. Comino, and H. L. Swinney (2017). Internal wave generation by tidal flow over periodically and randomly distributed seamounts, J. Geophys. Res. Oceans, 122, doi:10.1002/2017JC012884.

Zhao, Z., M. H. Alford, J. B. Girton, L. Rainville, and H. L. Simmons (2016). Global observations of open-ocean mode 1 M2 internal tides, J. Phys. Oceanogr., 46, 1657–1684, doi:10.1175/JPO-D-15-0105.1.